Slip detection methods and slip direction estimation on Quadruped Robots*

Paulo Teixeira Vale de Carvalho [1], **Vivian Suzano Medeiros**[2] **(Co-advisor), Marco Antonio Meggiolaro**[1] **(Advisor)**

[1]Pontifical Catholic University of Rio de Janeiro, Gávea, Rio de Janeiro, RJ, 22451-900, Brazil

[2]USP - São Carlos

pauloteixeiravc96@gmail.com, viviansuzano@usp.br, meggi@puc-rio.br

Abstract. *Quadruped robots are mobile robots inspired by the locomotion of animals. Although widely studied, challenges such as slip events remain significant. This work compares existing proprioceptive slip detection methods and evaluates a strategy for reducing undesirable detections. A slip direction estimation method is proposed for calculating a filtered slip angle to assess slip behavior and explore its potential as a criterion for slip intensity. To validate the approach, simulations and experiments are conducted using the Go1 robot. Results include a quantitative evaluation of slip detection methods based on the friction cone model, demonstrating consistent outcomes between simulation and experimental data, as well as a correlation between slip angle and slip intensity.*

Keywords. *Slip, Quadruped, Slip Detection, Slip Direction*

Info: *Student Level: Master*
Thesis defended on May 16th, 2025.
Submission to CTDR.

1. Introduction

Quadruped robots offer significant mobility advantages compared to wheeled or tracked robots, particularly in complex terrains. Their four-legged design provides greater stability than bipeds and more straightforward mechanics and energy efficiency relative to hexapods or octopods [Taheri and Mozayani 2023]. However, slippage remains a critical issue, often caused by the violation of friction constraints at foot contacts. This phenomenon can impair stability, disrupt sensor accuracy, and even cause physical damage. Thus, effective detection and management of slippage are crucial for robust quadruped locomotion.

Existing slip detection methods utilize exteroceptive and proprioceptive sensors, as well as specialized foot mechanisms. Despite various approaches, a gap remains in comprehensive comparisons among these methods and a detailed characterization of slip events, particularly regarding their direction and intensity. This work addresses these gaps by analyzing and comparing slip detection techniques, proposing improvements to reduce false positives, and introducing methods to estimate slip direction for enhanced locomotion control.

[1]This study was financed in part by the Coordenação de Aperfeiçoamento de Pessoal de Nível Superior - Brasil (CAPES), in part by Fundação de Amparo à Pesquisa do Estado do Rio de Janeiro (FAPERJ), and in part by the Brazilian National Research Council (CNPq).

2. Related Work

Various approaches exist to handle slippage in legged robots. Passive methods enhance robustness without explicit slip detection through mechanical design, robust control strategies, and terrain-aware state estimation. Examples include adaptive and bio-inspired foot designs [Wang et al. 2024, Yeom et al. 2024], optimization-based control and reinforcement learning strategies [Sim et al. 2020, Gangapurwala et al. 2022], and sensor fusion techniques in state estimation [Teng et al. 2021, Kim et al. 2022, Wisth et al. 2023].

Explicit slip detection methods rely on both proprioceptive and exteroceptive sensors, as well as specialized foot sensors. The literature indicates an advantage in the proprioceptive category, as it contains components with low latency that require less computational power compared to exteroceptive systems. Deterministic approaches integrate foot acceleration, analyze force drops, or set velocity thresholds [Focchi et al. 2018, Nisticò et al. 2022, Yoon et al. 2024]. Probabilistic methods use Hidden Markov Models for improved robustness [Jenelten et al. 2019], while recent machine learning techniques employ neural networks for advanced slip classification [Sun et al. 2023].

Beyond detection, slip characterization can provide essential information, such as friction coefficients and terrain classification, supporting adaptive locomotion strategies [Focchi et al. 2018, Zhang et al. 2023, Kim et al. 2025, Su et al. 2024]. However, detailed analyses focusing explicitly on slip direction and intensity are still limited, underscoring the need for further investigation, which is addressed in this work.

3. Slippage in Legged Robots

Legged robots are modeled as floating-base systems, where the base's motion depends entirely on external contact forces rather than direct actuation. This modeling typically introduces a fictitious joint with six degrees of freedom to represent the un-actuated floating base, allowing the use of standard Newton-Euler dynamics to describe robot motion [Hutter et al. 2017, Siciliano et al. 2010]. The general equations of motion are given by:

$$\boldsymbol{M}(\boldsymbol{q})\ddot{\boldsymbol{q}} + \boldsymbol{b}(\boldsymbol{q}, \dot{\boldsymbol{q}}) + \boldsymbol{g}(\boldsymbol{q}) = \boldsymbol{S}^T\boldsymbol{\tau} + \boldsymbol{J}_c^T\boldsymbol{F}_c, \tag{1}$$

where $\boldsymbol{q}$ contains both base and joint coordinates, $\boldsymbol{M}$ is the generalized mass matrix, $\boldsymbol{b}$ includes Coriolis and centrifugal terms, and $\boldsymbol{g}$ represents gravitational forces. Here, $\boldsymbol{\tau}$ denotes actuated joint torques, $\boldsymbol{S}$ selects actuated joints, and $\boldsymbol{J}_c$ maps ground reaction forces (, such asGRF) $\boldsymbol{F}_c$ from Cartesian to generalized coordinates.

Ground reaction forces, essential for robot locomotion, have normal (F_n) and frictional (F_f) components. The frictional force, which provides traction, must lie within the friction cone defined by Coulomb friction: $F_f \leq \mu F_n$, where μ is the static friction coefficient [Kao et al. 2008]. If this constraint is violated, slippage occurs.

Slippage negatively affects robot stability, sensor accuracy, control reliability, and can cause mechanical stress. Control strategies typically assume no-slip conditions, making slippage particularly problematic. Robust locomotion requires incorporating friction-aware contact planning or terrain estimation, though conservative assumptions limit performance. Active slip detection enables timely corrective actions, striking a balance between robustness and agility, and facilitating adaptive responses in uncertain terrain.

4. Methodology

4.1. Slip Detection Methods

This work compares four proprioceptive slip detection methods known for clear replicability and straightforward implementations: three deterministic methods [Focchi et al. 2018, Nisticò et al. 2022, Yoon et al. 2024] and one probabilistic approach [Yan et al. 2024]. Focchi et al. [Focchi et al. 2018] estimate slip occurrence by projecting the foot velocity onto the horizontal plane and applying adaptive thresholds that account for stance phase dynamics, aiming to distinguish true slip from normal oscillations in contact. Nisticò et al. [Nisticò et al. 2022] use combined thresholds on foot velocity and position deviations from planned trajectories to identify slippage events accurately. Yoon et al. [Yoon et al. 2024] distinguish slip conditions by applying thresholds to both foot velocity and acceleration, categorizing stance foot contacts into dynamic, static, or stable, thereby enhancing detection reliability within a state estimation framework. Yan et al. [Yan et al. 2024] adopt a probabilistic model, calculating slip likelihood based on displacement and tangential velocity, which is then processed through an empirically tuned error function.

To handle unwanted slip detections commonly observed during stance-to-swing transitions, particularly foot touchdown, the R-Filter is proposed. This method evaluates slips by defining the following slip-to-transition velocity ratio:

$$R_i = \frac{(A\boldsymbol{v}^b_{i_{xy}})^2}{|\boldsymbol{v}^b_{i_z}| + B}, \tag{2}$$

where $\boldsymbol{v}^b_{i_{xy}}$ is the tangential foot velocity and $\boldsymbol{v}^b_{i_z}$ is the vertical foot velocity. Parameters A and B are empirically set, creating a conservative filter that effectively reduces false-positive slip detections during transitional movements without sacrificing sensitivity to considerable slips.

4.2. Slip Direction Estimation

Accurately estimating slip direction provides additional context to detected slips, aiding responsive control. The proposed slip direction estimation method involves projecting the slip velocity onto a locally estimated terrain plane and computing its angle relative to the robot's heading direction. Terrain estimation uses a least-squares fit based on recent foothold positions, defining a terrain-aligned coordinate frame.

The slip angle θ_i is computed as:

$$\theta_i = \cos^{-1}\left(\frac{\langle {}^T\boldsymbol{v}_f, {}^T\mathbf{X}_b\rangle}{|{}^T\boldsymbol{v}_f| \cdot |{}^T\mathbf{X}_b|}\right), \tag{3}$$

where ${}^T\boldsymbol{v}_f$ represents the foot velocity in the terrain frame, and ${}^T\mathbf{X}_b$ is the terrain-projected forward direction of the robot base.

An Exponential Moving Average (EMA) filter smooths rapid fluctuations in slip angle estimates for clearer interpretation and real-time application:

$$\theta_i^f[k] = \alpha\,\theta_i[k] + (1-\alpha)\,\theta_i^f[k-1], \tag{4}$$

where α adjusts between smoothness and responsiveness, ensuring suitability for online robot control.

5. Results

5.1. Simulation Framework

The slip detection methods and the proposed improvements were validated through simulations using the quadruped robot Go1 from Unitree Robotics, implemented with the motion planning and control framework developed by Medeiros et al. [Medeiros et al. 2024]. This framework integrates Model Predictive Control (MPC) for trajectory optimization, Whole-Body Control (WBC) for joint torque computation, and a Kalman filter for state estimation, utilizing proprioceptive sensors only (Figure 1). Simulations were conducted in Gazebo, employing the ODE physics engine.

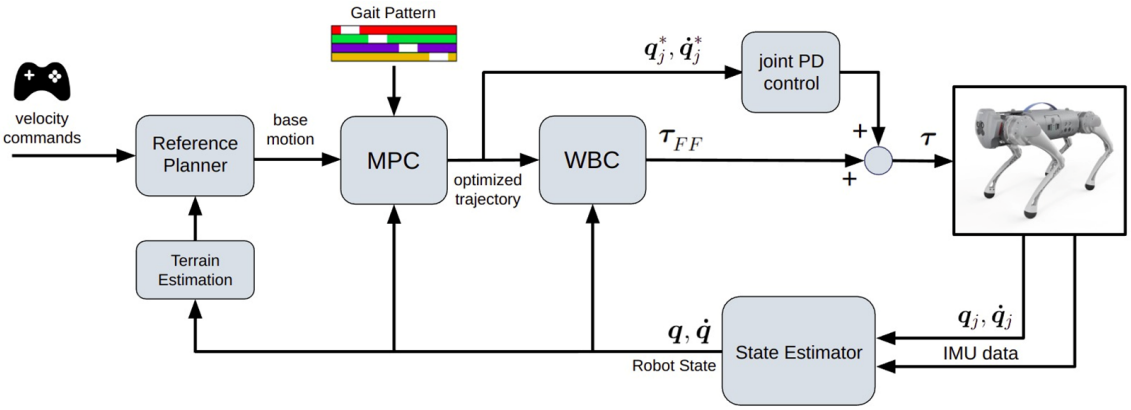

Figure 1. Diagram of the control and planning framework used for the Go1 robot simulations. Adapted from [Medeiros et al. 2024].

In this results section, simulations using the dynamic *Trot* and *Static Walk* gaits on an *Ice Patch* terrain scenario are presented. This scenario features a flat surface with a localized region of low friction (friction coefficient = 0.1), which is ideal for evaluating slip detection accuracy, the effectiveness of the proposed filter, and slip direction estimation. Further results involving simulations on a Slope are presented in the central thesis.

Few studies quantitatively compare slip detection methods. Sun et al. [Sun et al. 2023] report accuracy and recall but omit false positives, which are key to avoiding unnecessary responses. This work adopts a flag classification: positive matches (PM), false negatives (FNM), false positives (FPM), and negative matches (NM). It is expressed as occurrence percentages to quantify results. Combined with friction cone analysis, this approach offers a clearer basis for comparison, while robustness improvements remain for future work.

5.2. Performance Comparison for slip detection methods

In the Static Walk on the slippery surface, Focchi et al.'s method flags slips throughout all three stance phases. As shown in Figure 2, it briefly flags at stance onset, then continuously from the second V_{fxy} peak until swing-up. Even in mid-stance regions without ground truth slip, it often returns a continuous flag, likely due to low V_{fxy} or V_{fz} values, which keep the stance velocity below the median threshold.

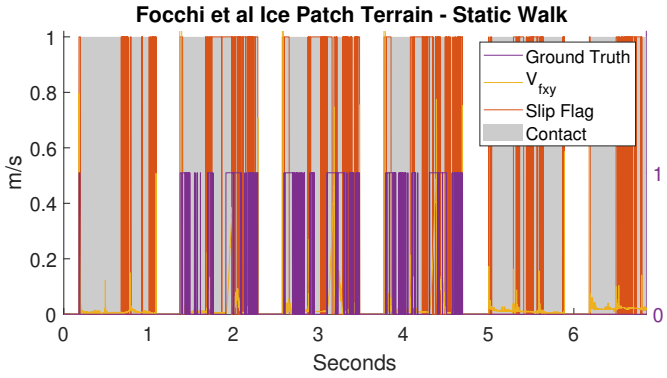

Figure 2. Slip detection with Focchi et al.'s method on Ice Patch Terrain (Static Walk).

Nisticò et al.'s method (Figure 3) concentrates slip flags around V_{fxy} peaks, showing a more conservative detection pattern. This may stem from its more complex formulation and the lower thresholds adopted due to MPC influence, which adjusts foot position and velocity. Even with smaller thresholds—usually linked to higher sensitivity—it remains the least sensitive in this setup, likely due to MPC interference on its inputs.

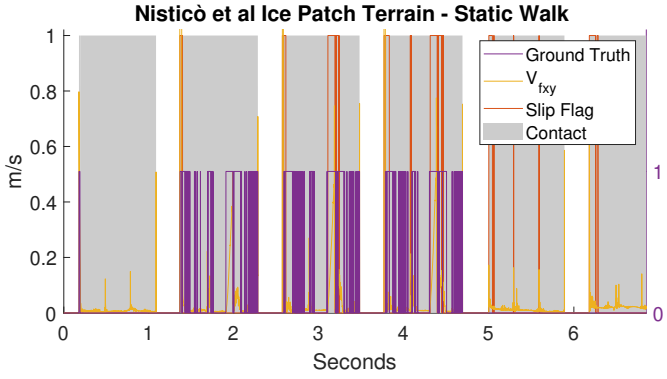

Figure 3. Slip detection with Nisticò et al.'s method on Ice Patch Terrain (Static Walk).

Figures 4 and 5 show that Yoon et al. and Yan et al. maintain their characteristic behavior, but with more frequent slip flags on the slippery surface. Yan et al.'s method also flags slips as the robot stops, indicating greater sensitivity to motion cessation than the others.

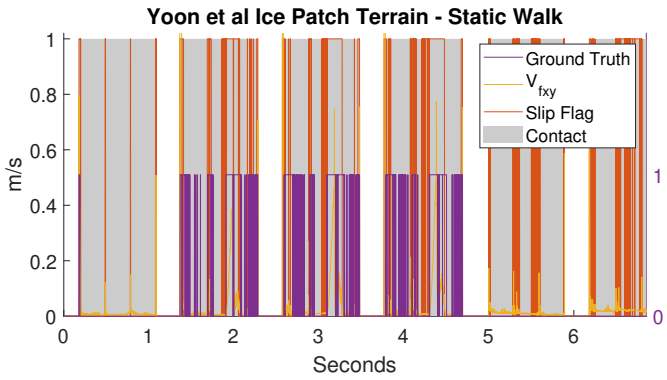

Figure 4. Slip detection with Yoon et al.'s method on Ice Patch Terrain (Static Walk).

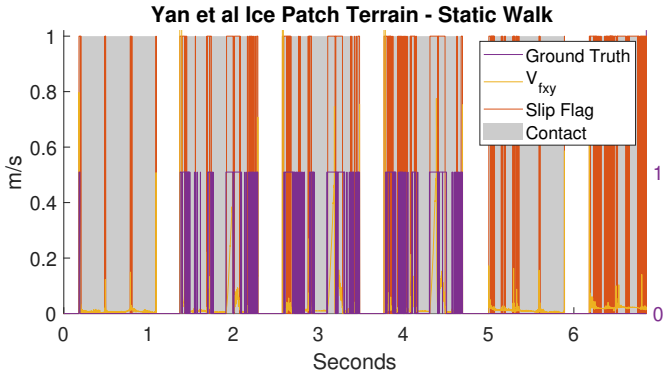

Figure 5. Slip detection with Yan et al.'s method on Ice Patch Terrain (Static Walk).

Table 1 shows Nisticò et al. with the lowest value (5.01%). PM rises for Focchi et al. and Nisticò et al., likely due to more intense slip events, whereas Yoon et al. and Yan et al. show a decrease, possibly because higher noise affects these more sensitive methods. Yan et al. still achieve the highest PM (66.75%) and a competitive FPM (16.03%), indicating consistent performance across terrains.

Ice Patch Terrain - Static Walk				
Ground Truth	**Slippage**	1134	**No Slippage**	3974
Methods	**PM%↑**	**FNM%↓**	**FPM%↓**	**NM%↑**
Focchi et al.	56.44	43.56	35.05	64.95
Nisticò et al.	29.19	70.81	**5.01**	94.99
Yoon et al.	57.80	42.20	13.05	86.95
Yan et al.	**66.75**	33.25	16.03	83.97

Table 1. Performance metrics on Ice Patch (Static Walk).

In the Trot gait scenario, Nisticò et al.'s method outperforms its results in previous cases. Figure 6 shows detections during the instability region, the preceding stance phase, and the residual instability after crossing, indicating that—even with generally more conservative behavior—it responds effectively to intense slip events or slip risks.

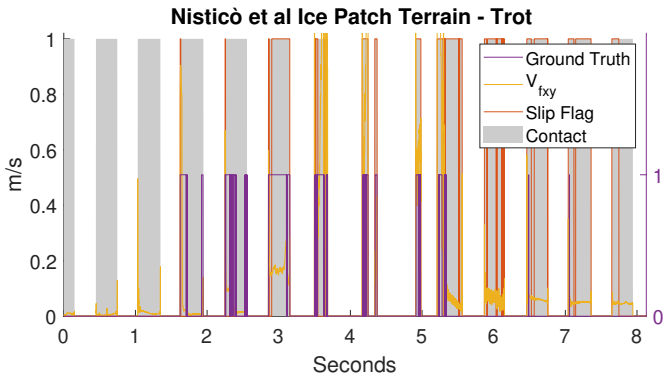

Figure 6. Slip detection with Nisticò et al.'s method on Ice Patch Terrain (Trot).

Figures 7 and 8 show that Yoon et al.'s and Yan et al.'s methods yield similar results, with identical slip flags during the crossing and longer responses to residual instability after it, reflecting their higher sensitivity compared to Nisticò et al.

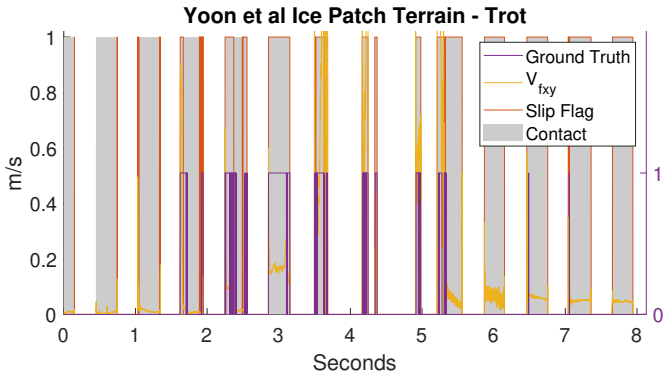

Figure 7. Slip detection with Yoon et al.'s method on Ice Patch Terrain (Trot).

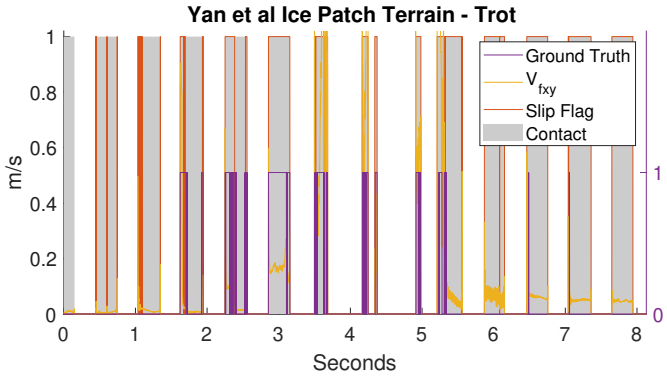

Figure 8. Slip detection with Yan et al.'s method on Ice Patch Terrain (Trot).

Table 2 shows that the Trot gait on the Ice Patch leads to higher PM and FPM than in the Static Walk case (Table 1), reflecting the scenario's greater instability. Yan et al. reach the highest PM (94.23%), while Nisticò et al. have the lowest PM (57.71%) and

FPM (46.85%). As seen in Figure 6, Nisticò et al.'s flags align with the most unstable moments, enabling timely reactions while avoiding excessive slip responses.

Ice Patch Terrain - Trot				
Ground Truth	**Slippage**	846	**No Slippage**	26490
Methods	**PM%↑**	**FNM%↓**	**FPM%↓**	**NM%↑**
Nisticò et al.	57.71	42.29	**46.85**	53.15
Yoon et al.	91.17	8.83	61.61	38.39
Yan et al.	**94.23**	5.77	60.05	39.95

Table 2. Performance metrics on Ice Patch (Trot).

The R-Filter was tested with Nisticò et al.'s method on the Ice Patch (Trot) using a period $t_{tr} = 52.26\,\text{ms}$. As shown in Figure 9, it reduced FPM from 21.93% to 3.82% in the applied period, preserving only significant slip events and enhancing the relevance of Nisticò et al.'s key detections.

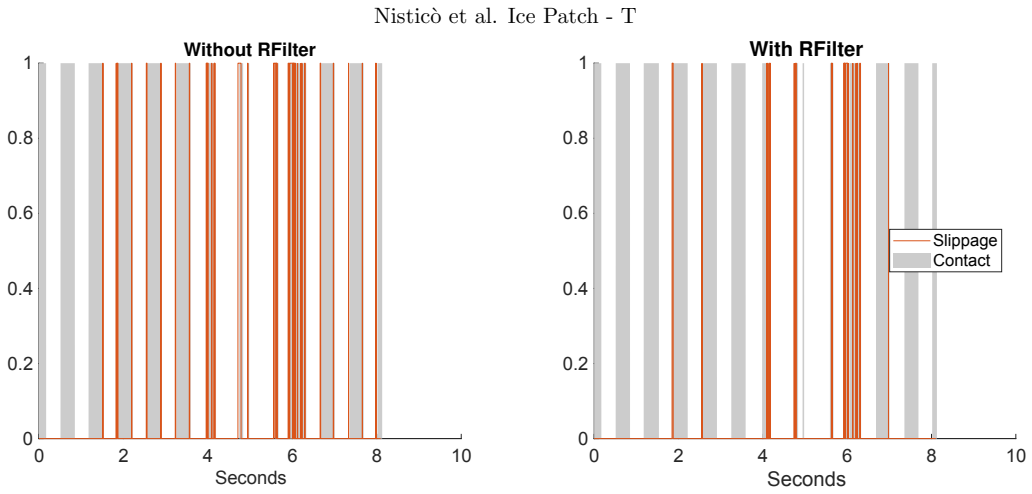

Figure 9. Comparison of Nisticò et al.'s method with and without R-Filter.

5.3. Slip direction results

Figures 10 and 11, for Static Walk and Trot on the Ice Patch, show notable slip angle variation when the foot crosses the Ice Patch. In Static Walk, oscillations linked to V_{fxy} peaks vary in amplitude between 1 and 5 seconds, indicating sideways slip and instability. In Trot, a sharp oscillation between 1.5–2 s during touchdown and lift-off is followed by a consistent rightward bias from 2 to 5 seconds, suggesting reduced ability to correct foot placement.

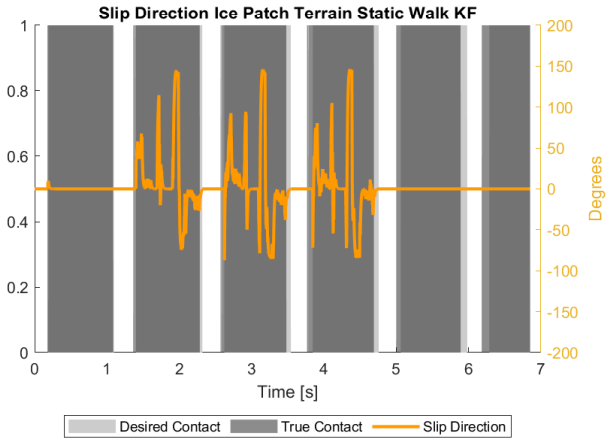

Figure 10. Slip direction estimation using ground truth data (Ice Patch).

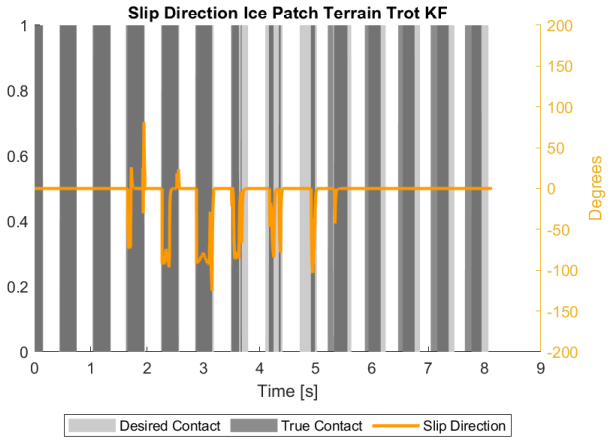

Figure 11. Slip direction estimation using Kalman Filter data (Ice Patch).

A slip angle oscillating around zero, as in Figure 10, or consistently biased to one side, as in Figure 11, may indicate distinct slip scenarios. Understanding these patterns can help develop more effective strategies for slip classification and response.

5.4. Experiment

The experimental dataset consists of three trials, each recorded with synchronized proprioceptive data and video footage. Among these, the third trial was selected for detailed presentation in this paper, as it better represents the conditions and behavior of interest for slip detection and slip direction estimation. In this trial, the robot falls on its first attempt to cross the slippery plate, producing clear slip events and recovery attempts that are suitable for evaluating the proposed methods.

Figure 12 shows snapshots from Sample 3, where the Go1 robot steps onto the slippery surface, loses stability, and eventually falls. This visual reference supports the

analysis in Figure 13, where Yan et al.'s method shows less tendency to flag slip during foot phase transitions outside the slippery zone, while behaving similarly within it.

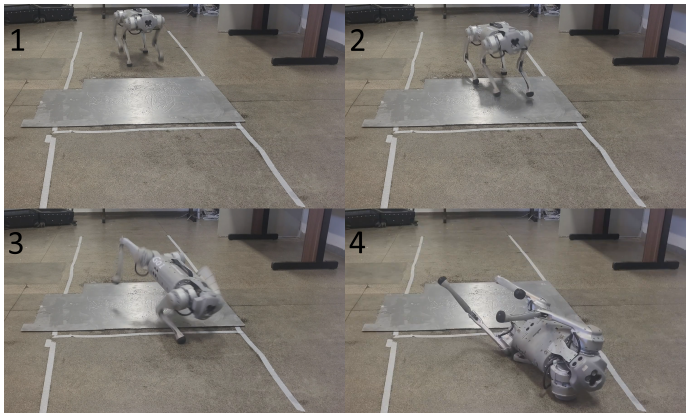

Figure 12. Snapshots of Go1 falling on the slippery plate (Sample 3).

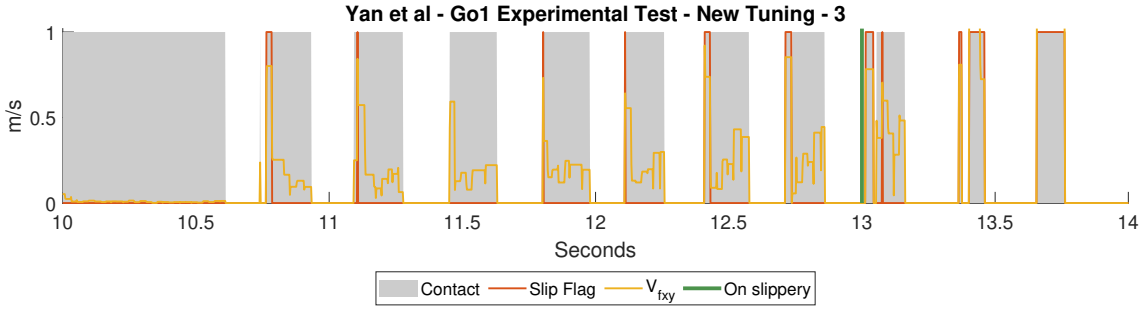

Figure 13. Slip detection with Yan et al.'s method on Sample 3, using retuned parameters.

Figure 14 presents the slip angle estimation for the same trial. Positive angles correspond to outward sliding relative to the Front Left foot. In this case, the main slip event starts shortly after the green marker (foot stepping onto the slippery plate) and matches the destabilization seen in the video (Figure 12). The oscillations in slip angle during the recovery phase are consistent with the robot's unsuccessful stabilization attempts before falling.

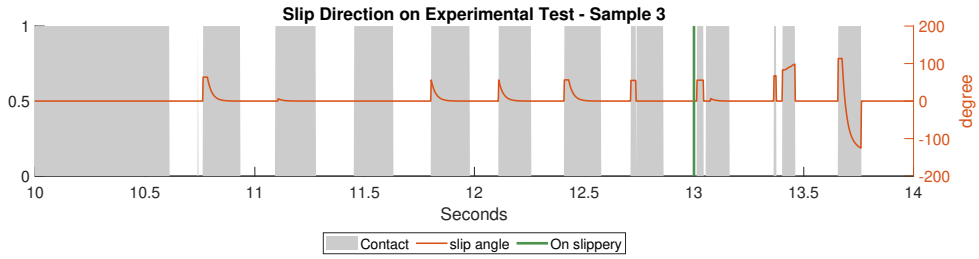

Figure 14. Slip angle estimation on Sample 3, using Yan et al.'s detection to trigger the estimator.

Overall, the results show that both slip detection and slip direction estimation perform consistently with qualitative video observations. The proposed slip angle estimator produces smooth and interpretable curves even under experimental noise, reinforcing its applicability to real-world conditions.

6. Conclusion

This paper compared proprioceptive slip detection methods in quadruped robots and proposed two contributions: an R-Filter to reduce false positives during foot transitions and a slip direction estimator based on the slip angle. Both were tested in twelve simulation configurations and validated with experimental data. Among the evaluated methods [Nisticò et al. 2022, Focchi et al. 2018, Yoon et al. 2024, Yan et al. 2024], Nisticò et al. achieved the lowest false positive rate, while Yan et al. adapted better to real scenarios. The R-Filter suppressed noise during swing-stance transitions, and the low-pass filter improved slip angle interpretability. The slip direction estimator also captured trends consistent with terrain irregularities, even without force sensing.

Future research should focus on real-time validation of the R-Filter and low-pass filter to assess their performance under operational conditions, as well as the development of a slip reaction module that leverages slip angle feedback to optimize detection accuracy while minimizing false positives. Exploring robust ground truth baselines, such as force plates, visual tracking, and cross-comparisons between simulation physics engines, could improve validation reliability. Additionally, combining multiple detection methods, refining proprioceptive indicators to include slip cause and intensity, and adapting these approaches to other legged morphologies or hybrid legged-wheeled platforms may enhance robustness, adaptability, and overall applicability across diverse locomotion scenarios.

References

Focchi, M., Barasuol, V., Frigerio, M., Caldwell, D. G., and Semini, C. (2018). Slip detection and recovery for quadruped robots. *Springer Proceedings in Advanced Robotics*, 3:185–199.

Gangapurwala, S., Geisert, M., Orsolino, R., Fallon, M., and Havoutis, I. (2022). Rloc: Terrain-aware legged locomotion using reinforcement learning and optimal control. *IEEE Transactions on Robotics*, 38:2908–2927.

Hutter, M., Siegwart, R., Stastny, T., Rudin, K., and Blösch, M. (2017). Robot dynamics lecture notes. Available at: `https://ethz.ch/content/dam/ethz/special-interest/mavt/robotics-n-intelligent-systems/rsl-dam/documents/RobotDynamics2017/RD_HS2017script.pdf`. Accessed: April 2025.

Jenelten, F., Hwangbo, J., Tresoldi, F., Bellicoso, C. D., and Hutter, M. (2019). Dynamic locomotion on slippery ground. *IEEE Robotics and Automation Letters*, 4:4170–4176.

Kao, I., Lynch, K., and Burdick, J. W. (2008). *Contact Modeling and Manipulation*, pages 647–669. Springer Berlin Heidelberg, Berlin, Heidelberg.

Kim, H., Kang, D., Kim, M. G., Kim, G., and Park, H. W. (2025). Online friction coefficient identification for legged robots on slippery terrain using smoothed contact gradients. *IEEE Robotics and Automation Letters*, 10:3150–3157.

Kim, Y., Yu, B., Lee, E. M., Kim, J. H., Park, H. W., and Myung, H. (2022). Step: State estimator for legged robots using a preintegrated foot velocity factor. *IEEE Robotics and Automation Letters*, 7:4456–4463.

Medeiros, V. S., Escalante, F. M., Becker, M., and Boaventura, T. (2024). Impedance control analysis for legged locomotion in oscillating ground. In Youssef, E. S. E., Tokhi, M. O., Silva, M. F., and Rincon, L. M., editors, *Synergetic Cooperation between Robots and Humans*, pages 197–208, Cham. Springer Nature Switzerland.

Nisticò, Y., Fahmi, S., Pallottino, L., Semini, C., and Fink, G. (2022). On slip detection for quadruped robots. *Sensors*, 22:1–14.

Siciliano, B., Sciavicco, L., Villani, L., and Oriolo, G. (2010). *Robotics: Modelling, Planning and Control*. Springer Publishing Company, Incorporated.

Sim, O., Jeong, H., Oh, J., Lee, M., Lee, K. K., Park, H. W., and Oh, J. H. (2020). Joint space position/torque hybrid control of the quadruped robot for locomotion and push reaction. *Proceedings - IEEE International Conference on Robotics and Automation*, pages 2450–2456.

Su, Y., Yang, H., Ding, L., Xu, C., Xu, P., Gao, H., Niu, L., Li, W., Liu, G., and Deng, Z. (2024). A unified foot-terrain interaction model for legged robots contacting with diverse terrains. *IEEE/ASME Transactions on Mechatronics*, 29:2661–2672.

Sun, P., Qiang, J., Qian, L., and Luo, X. (2023). Learning slip detection for agile locomotion of quadruped robots. *2023 IEEE International Conference on Robotics and Biomimetics, ROBIO 2023*, pages 1–6.

Taheri, H. and Mozayani, N. (2023). A study on quadruped mobile robots. *Mechanism and Machine Theory*, 190:105448.

Teng, S., Mueller, M. W., and Sreenath, K. (2021). Legged robot state estimation in slippery environments using invariant extended kalman filter with velocity update. *Proceedings - IEEE International Conference on Robotics and Automation*, 2021-May:3104–3110.

Wang, H., Liu, P., Chen, H., Ngoc, P. T. T., Li, B., Li, Y., and Sato, H. (2024). Toward the smooth mesh climbing of a miniature robot using bioinspired soft and expandable claws. *IEEE Transactions on Medical Robotics and Bionics*, 6:351–361.

Wisth, D., Camurri, M., and Fallon, M. (2023). Vilens: Visual, inertial, lidar, and leg odometry for all-terrain legged robots. *IEEE Transactions on Robotics*, 39:309–326.

Yan, C., Qin, J., Liu, Q., and Ma, Q. (2024). Slip detection and recovery for quadruped robots via orthogonal decomposition. *IEEE Transactions on Industrial Electronics*.

Yeom, H., Park, G., and Bae, J. (2024). Design of a human-inspired sensorized and adaptive foot that enhances stability through tensegrity (hi-safest). *IEEE Robotics and Automation Letters*, 9:4305–4312.

Yoon, Z., Kim, J. H., and Park, H. W. (2024). Invariant smoother for legged robot state estimation with dynamic contact event information. *IEEE Transactions on Robotics*, 40:193–212.

Zhang, Z., An, H., Wei, Q., and Ma, H. (2023). Learning-based model predictive control for quadruped locomotion on slippery ground. pages 47–52.